On Wet Etching of n-Si (100) Coated with Sparse Ag-Particles in Aqueous NH$_4$F with the Aid of H$_2$O$_2$

C. L. Chuang[2], J. C. Lin[1,2,*], K. H. Chao[2], C. C. Lin[3] , G. Lerondel[3]

[1] Institute of Materials Science and Engineering, Central University, No.300, Jhongda Rd., Jhongli City, Taoyuan County 320, Taiwan
[2] Department of Mechanical Engineering, National Central University, No.300, Jhongda Rd., Jhongli City, Taoyuan County 320, Taiwan
[3] Laboratoire de Nanotechnologies et d'Instrumentation Optique, ICD, CNRS Université de Technologie de Troyes, 12 rue Marie Curie BP2060 10010 Troyes cedex, France
[*]E-mail: jclin4046@gmail.com

Single crystalline n-Si (100) previously coated with sparse silver nano-particles were immersed in various solutions of ammonium fluoride to investigate their wet etching. In the absence of H$_2$O$_2$, the open circuit potential (OCP) of the silicon was more active in the solutions of 11.0 M than 1.0 M NH$_4$F. In the present of H$_2$O$_2$, the OCP of the silicon increased with increasing the concentration of H$_2$O$_2$ (from 1.0 to 5.0 M). The etching morphology of the specimens, examined through scanning electron microscopy (SEM), revealed two different types. The first type of morphologies revealed a number of deep pores produced on the n-Si (100) post its immersion in 1.0 M NH$_4$F + 5.0 M H$_2$O$_2$ for 1 h. These pores were 50 - 150nm in diameter and 200 - 300nm in depth. The second type of morphologies displayed few shallow pores on the Si (100) post its immersion in 11.0 M NH$_4$F + 5.0 M H$_2$O$_2$ for 1 h. The study of electrochemical impedance spectroscopy (EIS) provided useful information to understand the kinetics of this system. The experimental EIS data simulated with commercial software (i.e., Z-view) were satisfactorily consistent with two distinct sets of proposed equivalent circuit (i.e., EQA and EQB) in response to those two different etching morphologies. Based on EQB, we construct a schematic model to illustrate the formation of deep pores on n-Si (100) in the system of 1.0 M NH$_4$F + 5.0 M H$_2$O$_2$. The oxide capacitance (i.e., C$_1$) present in EQB is absent in EQA and replaced with an inductance (i.e., L$_1$). EQA could be used to delineate the kinetics of n-Si (100) in two single solutions of 1.0 and 11.0 M NH$_4$F and that in 11.0 M NH$_4$F + 5.0 M H$_2$O$_2$. In the absence of H$_2$O$_2$, the charge-transfer resistance (i.e., R$_2$) in EQA is very high so that n-Si (100) is highly resistant to corrosion in both single 1.0 and 11.0 M NH$_4$F. However, in the presence of H$_2$O$_2$, this charge transfer (i.e., R$_2$) is hugely reduced in the system of 1.0 M NH$_4$F + 5.0 M H$_2$O$_2$ and 11.0 M NH$_4$F + 5.0 M H$_2$O$_2$. The contribution of hydrogen peroxide is not only to increase the open circuit potential but also to facilitate the creation of holes in the catalytic process assisted by the sparse nano Ag-particles on the n-Si (100) surface. The mechanism could be confirmed by the plots of phase angle against the exerted frequencies.

1. INTRODUCTION

Porous silicon was first discovered by Uhlir in 1956 [1], following which many studies on the mechanisms underlying the formation and responses of porous silicon were conducted. Initially, porous silicon was employed mostly as a sacrificial layer. In 1990, Lehmann fabricated porous silicon structures with high aspect-ratios [2], whereupon applications of porous silicon expanded to micro electro-mechanical systems (MEMS) [3-5], thin film technologies [6], detectors [7], and optoelectronic materials. In these areas, the etching techniques for n-type silicon require a specific anode bias voltage and light irradiation in order to form pores.

In 2000, Li *et al*. [8] developed a metal-assisted approach to chemical etching. In their study, they deposited precious metals including platinum, gold, and palladium on silicon surfaces to function as metal catalysts. Wet etching was carried out by using a solution of hydrofluoric acid (49 %) and hydrogen peroxide (30 %) to produce a nano-porous layer without the need of applying electrical bias. In 2008, R. Douani *et al*. [9] employed a combination of silver reduction solution and an etching solution of highly concentrated hydrofluoric acid (22.5M HF / 0.05M $AgNO_3$ + 0.01M $Na_2S_2O_8$) to oxidize the surface of a silicon substrate and reduce the metal ions within the solution at 50 °C. Concurrent with the process of silver reduction, they successfully etched silicon nano wires in concentrated HF solution.

It was evident that hydrofluoric acid was the most common etching reagent used in metal-assisted wet etching solutions [10-12]. Oxidizers such as hydrogen peroxide or, in the case of highly concentrated hydrofluoric acid solutions, potassium dichromate, potassium bromate, or potassium iodate [13], may be added to the etching solution to oxidize the silicon substrate. It is believed that oxidizers accelerate the formation of silica which is more reactive than silicon to react with fluoride ions in the etching solution, thereby speeding up the etching process. Hydrofluoric acid or mixtures of hydrofluoric acid and ammonium fluoride are the most common commercial pre-treatments for silicon wafers; different ratios with varying pH values can be used to clean silicon wafers, remove SiO_2 layers, or achieve hydrogen termination, leaving wafer surfaces stable and free of impurities.

It is rational that the Ag-assisted wet etching on p-type silicon is more readily than that on n-type because of abundance of holes in the p-type silicon. Wet etching on n-type silicon usually should be undertaken under illumination because pairs of electron-hole could be induced by irradiation and separated. These holes present on the surface of n-type silicon enables the possible etching of the silicon [14].

As mentioned above, coating of noble metals on silicon and oxidation on the silicon surface led to accelerate the etching rate of silicon in hydrofluoric acid. However, the toxicity of hydrogen fluoride and its volatile vapor at room temperature is a risk to the industrial safety. Many efforts were devoted to develop etching solutions applicable to silicon with less toxicity. Ammonium fluoride was considered less toxic than hydrogen fluoride because of much lower vapor pressure at room temperature. However, very low reactivity is the main drawback of ammonium fluoride for its single use. Ammonium fluoride reveals a weak alkalinity (i.e., with a pH value of approximately 8 [15-16]) as the concentration up high to 40% (roughly at 11.0 M).

There were few reports dealing with silicon etching in ammonium fluoride solutions which could be accelerated by using anodic bias (i.e., assisted by anodic polarization) [17]. However, wet etching of n-type silicon assisted by previous deposition of noble metals in the ammonium fluoride was seldom reported. An attempt was made in the present work to explore the silver-assisted wet etching of the n-Si (100) in both the dilute (1.0 M NH_4F) and concentrated (11.0 M NH_4F) ammonium fluoride solutions to compare its etching kinetics. Prior to wet etching, silicon was first pre-treated in a bath of silver nitrate to coat with nano-scale Ag-particles that are sparely distributed on the top surface. The effect of oxidizers on the Ag-assisted wet etching of p-type silicon in hydrogen fluoride solution was well studied in the literature [11]. However, this effect on the Ag-assisted wet etching of n-type silicon in ammonium fluoride solutions had not yet reported. Due to this fact, we devoted ourselves to the Ag-assisted wet etching of n-Si(100) in alkaline fluoride solutions in dark condition to get rid of the interference of irradiation. The objective of this study was to investigate morphological change and etching kinetics for the silver-assisted wet etching of n-type (100) silicon in dilute (1.0 M NH_4F) and concentrated (11.0 M NH_4F) ammonium fluoride solutions containing whether or not 1.0 M and 5.0 M H_2O_2. Moreover, it was well known that electrochemical impedance spectroscopy (EIS) provided an excellent tool to realize the kinetics and reaction mechanism for the wet etching of silicon in acidic solutions [14]. EIS study on the etching mechanism of n-type silicon in alkaline solutions was rarely reported. The EIS of n-Si (100) in the alkaline fluoride solutions was of concern in this work.

2. EXPERIMENTAL DETAILS

Wafers of n-type (100) single crystal silicon doped with phosphorus, with their electrical resistivity at 10-20 Ω-cm, were used as the basic substrates for this etching study. They were sliced into specimens with the dimension 10×10 mm^2 in thickness of 525 μm. The specimens were cleaned in a sequence of fluids such as acetone, alcohol, and deionized water, etc. in conjunction with ultrasonic oscillation to remove the contaminants, grease and organic impurities on the silicon. After the cleaning processes which ended up with a flush of deionized water, the specimens were immersed in a solution of 1 % hydrofluoric acid for 30 s to prevent from the possible contamination by oxides on the surface. The specimen were finally removed and dried by using nitrogen gas.

For deposition of sparsely distributed silver nano-particles on the surface of silicon substrate, the silicon substrates were immersed in a 150 mL bath containing silver nitrate (2.0 mM) and 0.08 M formaldehyde at 20℃ for 10 minutes, then removed to proceed soft baking in an oven at 80℃ for 1 h to ensure the complete evaporation of the unreacted chemical reagents and moisture, thus resulted in a sparse distribution of nano-particles that attached firmly on the silicon surface.

The set-up and equipment used to investigate wet etching in the present work were shown in Fig. 1. An etching tank (80 x 50 x 60 cm^3) made of poly-tetrafluoroethylene (PTFE) to display an inner capacity of 150 ml. A circular hole with 9 mm in diameter (equal to an area of 64 mm^2) was located on the side of the tank to expose the surface of the Ag-deposited specimens to contact with the etching solution. The Ag-deposited specimen was fixed by a sample holder made of pure copper (99.90 %). An indium-gallium alloy was brushed onto the backside of the specimen to form an Ohmic contact with

the copper plate firmly fixed in the sample holder. A connecting lead with one end conducted to a potentiostat (Potentiostat/Galvanostat AutoLab EG&G2263) and the other end in connection to this sample holder to act as anode or working electrode. A piece of platinum (99.99 % pure) foil (dimension in 50 mm x 50 mm x 0.5 mm) was served as the counter electrode (i.e., cathode, or auxiliary electrode). A saturated calomel electrode (SCE) equipped with a salt bridge made of high density polyethylene (HDPE) capillary tube filled with saturated KCl solution employed as a reference electrode in this experiments. The potential data were reported against SCE in this work.

Dilute (1.0 M) and concentrated (11.0 M) ammonium fluoride (NH_4F) aqueous solutions were used as the etching solutions in which the pH was approximately 5 in the former and approximately 8 in the later. Hydrogen peroxide was free (0 M) or in the presence (1.0 M, and 5.0 M) to investigate the H_2O_2-effect on the wet etching kinetics of silicon. The experiments were carried out in ambient temperature and atmosphere. The open circuit potential (OCP) of the Ag-deposited specimens was determined against SCE with a potentiostat aforementioned in Fig. 1. Electrochemical impedance spectroscopy was applied to study the wet etching of the Ag-deposited n-Si (100) in various NH_4F solutions in the absence and presence of H_2O_2. For minimizing the possible interference caused by concentration polarization in the measuring EIS data, we stirred the solution with a magnetic stirrer to maintain solution circulation. In the performance of EIS measurement, the frequency was varied in a range from 10^5 Hz to 0.1 Hz at 5 points/decade with amplitude of 50 mV. By means of a commercial simulation software (Z-view, Schlumberger, England), we could proposed a number set of theoretical equivalent circuits possibly corresponding to different etching mechanism to simulate with the experimental EIS data. After ruling out the mechanisms governed by theoretical equivalent circuits which did not fit satisfactorily, we could propose a reasonable mechanism of this wet etching process. The surface morphology of silicon substrate and the Ag-deposited specimen before and post wet etching was examined by a field emission scanning electron microscope (FE-SEM, FEI-NNS230).
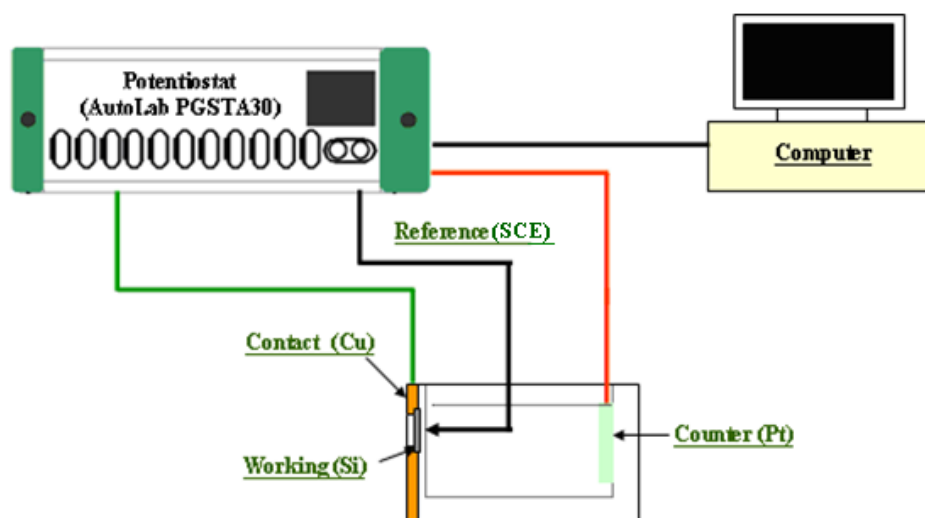

Figure 1. Schematic diagram for the experimental setup used in this work to conduct dark etching of Si deposited previously with sparse Ag-particles in the solutions of NH_4F in the absence and presence of H_2O_2.

3. RESULTS

3.1 The open circuit potential (OCP) for the Ag-deposited Si (100)

The open circuit potential (OCP) of the n-type Si (100) previously deposited with silver nanoparticles was measured in both dilute (1.0 M) and concentrated (11.0 M) ammonium fluoride (NH$_4$F) solution in the absence and presence of hydrogen peroxide varying in 1.0 and 5.0 M. Figure 2 depicted that in the absence of hydrogen peroxide, the OCP of Si (100) is more active in 11.0 M than 1.0 M NH$_4$F solution. The addition of hydrogen peroxide led to a shift of OCP to the noble direction. With increasing the concentration of H$_2$O$_2$, the OCP is getting higher. Almost all the OCP revealed a little fluctuation and stabilized within 10 minutes. The EIS study should be conducted at a stable OCP, at which only a small fluctuation (i.e., within ±10 mV) occurred. In the absence of H$_2$O$_2$, the OCP was stabilized at approximately -406 mV in 1.0 M NH$_4$F. In the presence of H$_2$O$_2$, the OCP increased with increasing the concentration of H$_2$O$_2$. It was -375 mV (in 1.0 M NH$_4$F + 1.0 M H$_2$O$_2$) and -368 mV (in 1.0 M NH$_4$F + 5.0 M H$_2$O$_2$), respectively. In contrast, in the concentrated (11.0 M) NH$_4$F solution, the OCP inclined to increase in the order -483 mV (11.0 M NH$_4$F) < -431 mV (11.0 M NH$_4$F + 1.0 M H$_2$O$_2$) < -386 mV (11.0 M NH$_4$F + 5.0 M H$_2$O$_2$). This fact implied that in the present oxidant like hydrogen peroxide (with its oxidation-reduction potential at +1.52V SCE) in the etching solution, the OCP of n-Si (100) was getting higher perhaps ascribed to oxidization of the silicon surface by hydrogen peroxide. The higher concentration of the hydrogen peroxide, the greater extent is the oxidation on the silicon.
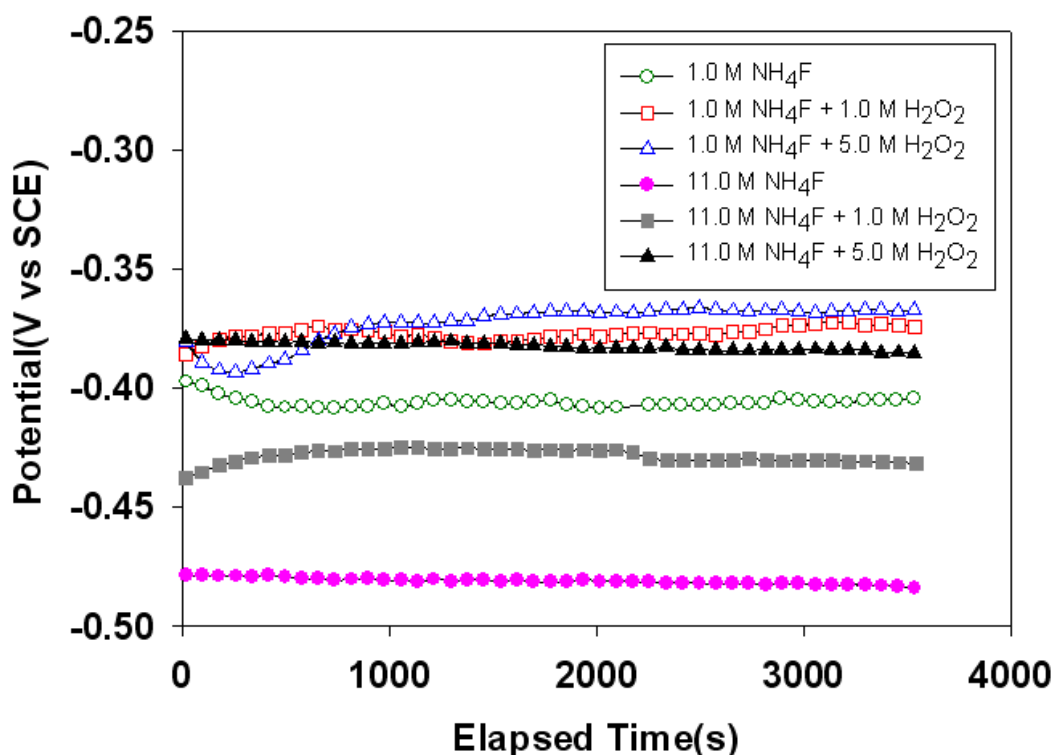

Figure 2. Open circuit potential measured in the dark etching of n-type Si(100) in a variety of 1.0 and 11.0 M NH$_4$F solutions containing in the absence and presence of 1.0 and 5.0 M H$_2$O$_2$

3.2 Surface morphology of n-Si (100) prior to and post wet etching

Prior to wet etching, the specimen of n-Si (100) was treated chemically in a bath of dilute $AgNO_3$ solution with nano-scale silver particles. Figure 3 depicted a top-view SEM image of the specimen. Evidently, the surface of n-Si (100) was uniformly coated with nano-particles, roughly 50 - 80 nm in diameter. Through examination the whole surface of the specimen with lower magnification mode of SEM, we found no presence of the islands or consecutive clusters of the particles. Elemental analysis by the attached energy dispersive spectrometer (EDS) indicated that these particles belong to metallic silver and the substrate is silicon.
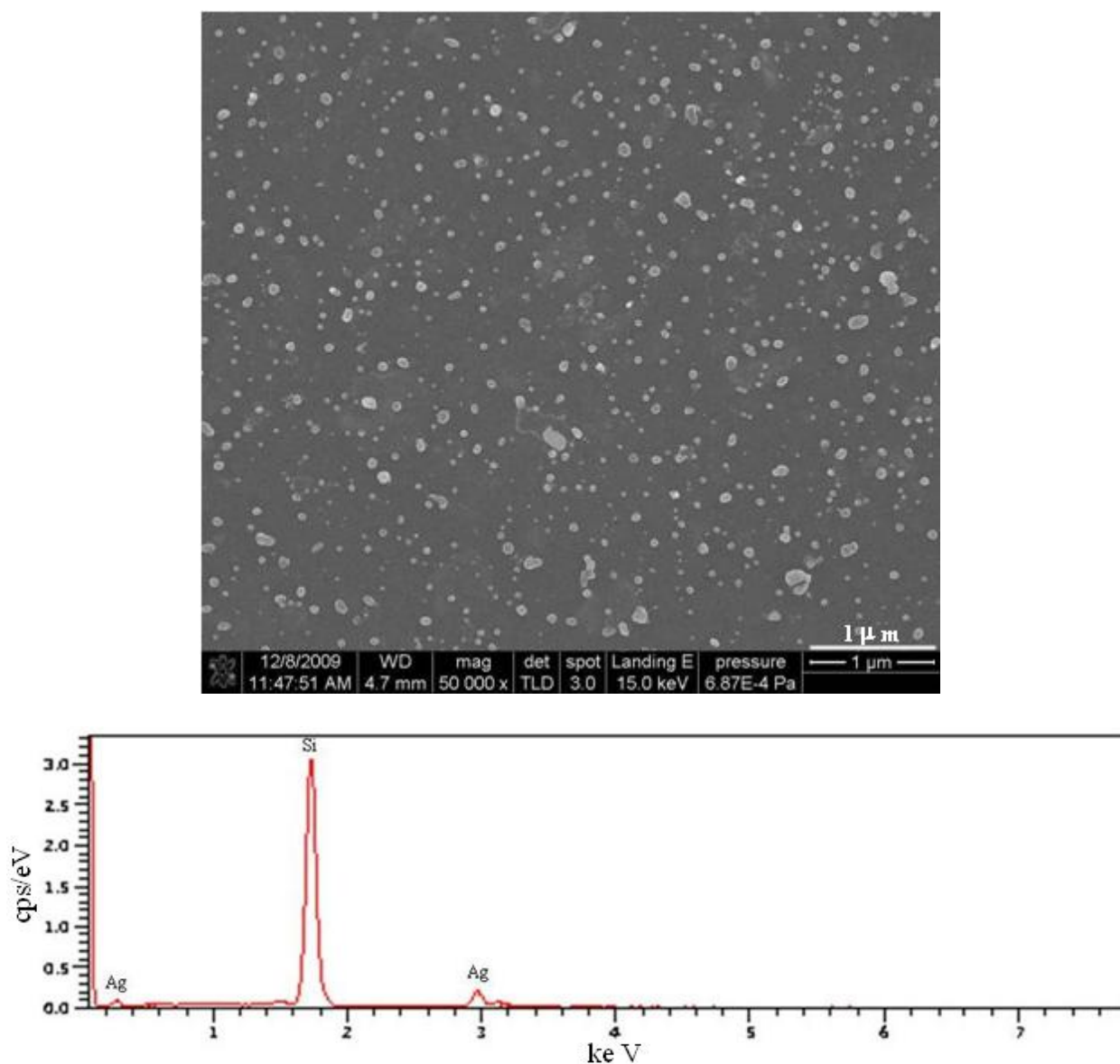

Figure 3. Micrograph of the scanning electron morphology (SEM) on the top surface of n-type Si(100) deposited previously in a bath of silver nitrate with its corresponding elemental analysis data of energy dispersive spectra (EDS).

Figure 4 displayed the top views of SEM for n-Si (100) post wet etching for 1 h in 1.0 M NH$_4$F aqueous solutions containing various concentrations of H$_2$O$_2$ (i.e., 0, 1.0 and 5.0 M) under lower magnification (x 50 k) in the left column and with higher magnification (x200 k) in the right column. In Figs. 4(a) and (d), the surface of n-Si (100) depicted a flat almost non-attack appearance post immersion in the simple 1.0 M NH$_4$F solution free from hydrogen peroxide for 1 h. This fact implies the silicon surface is nearly not attack by the dilute ammonium fluoride (i.e., 1M NH$_4$F) in the absence of H$_2$O$_2$. In contrast Fig. 4(a) to Figs. 4(b) and (c), it is seen that in the presence of H$_2$O$_2$, the surface of silicon suffer attack by 1.0 M NH$_4$F solution and the extent of attack depending upon the concentration of H$_2$O$_2$. A comparison between Figs. 4(b) and (c), also between Figs 4 (e) and (f), we found that a number of pores were formed on the surface of silicon post etching in a mixture of 1.0 M NH$_4$F with 1.0 and 5.0 M H$_2$O$_2$ for 1 h. The average diameter of the pores increases from 50 nm to 150 nm with increasing the H$_2$O$_2$ concentration from 1.0 to 5.0 M. By checking the etched morphologies, we found that many particles are still remained in the pores; whereas, a few of particles were dug out from the pores to lie aside. The pores were distributed on the silicon surface in the manner as the distribution of nano-scale silver particles before etching.
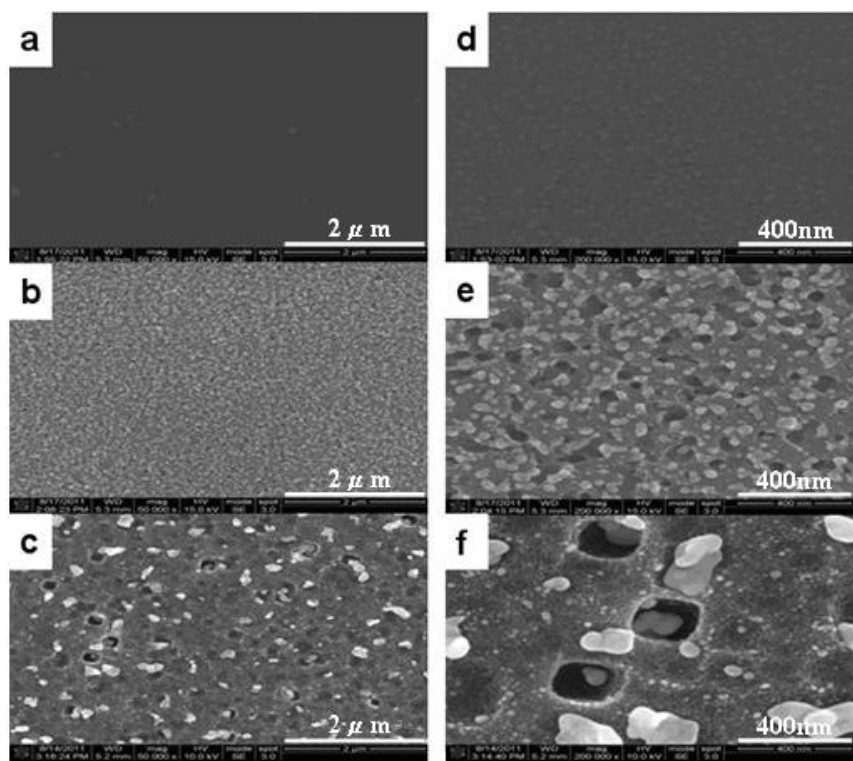

Figure 4. Top views of SE morphologies for n-Si specimen post dark etching for 1 h in 1.0 M NH$_4$F aqueous solutions containing (a) 0 (b) 1.0 (c) 5.0 M H$_2$O$_2$ with lower magnification (x 50 k) in the left column and those post dark etching for 1 h in 1.0 M NH$_4$F aqueous solutions containing (d) 0 (e) 1.0 (f) 5.0 M H$_2$O$_2$ with higher magnification (x 200 k) in the right column.

Figure 5 depicted the top views of SEM for n-Si (100) post wet etching for 1 h in very concentered ammonium fluoride aqueous solution (i.e., 11.0 M NH$_4$F) containing various

concentrations of H_2O_2 (i.e., 0, 1.0 and 5.0 M) under lower magnification (x 50 k) in the left column and with higher magnification (x200 k) in the right column. The morphology in Figs. 5(a) and (d) indicated that the surface of n-Si (100) also remained almost non-attack and distributed with silver particles after 1 h immersion in the monotonic 11.0 M NH_4F solution. This fact indicated that the attack of silicon in any concentration of ammonium fluoride is negligible in the absence of oxidant such as hydrogen peroxide. In comparison of Fig. 5(a) with Figs. 5(b) and (c), the effect of 1.0 M H_2O_2 present in 11.0 M NH_4F is nearly non-detected but the involvement of 5.0 M H_2O_2 is significant in 11.0 M NH_4F. In contrast to Figs. 5(b) and (c), also Figs 5 (e) and (f), we only found very shallow pores were formed on the surface of silicon after etching in a mixture of 11.0 M NH_4F with 5.0 M H_2O_2 for 1 h.
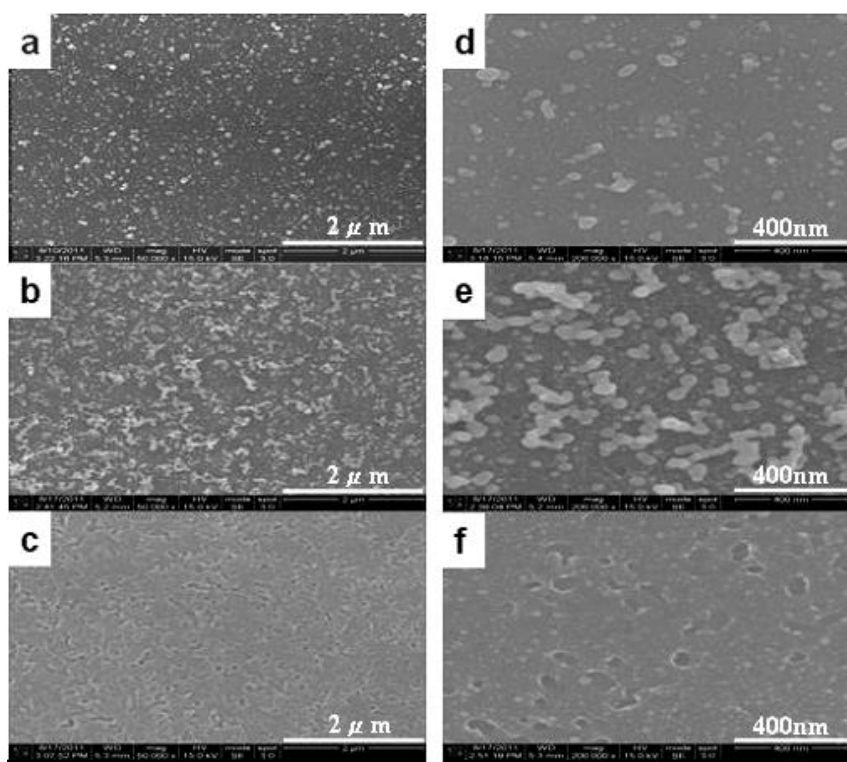

Figure 5. Top views of SE morphologies for n-Si specimen post dark etching for 1 h in 11.0 M NH_4F aqueous solutions containing (a) 0 (b) 1.0 (c) 5.0 M H_2O_2 with lower magnification (x 50 k) in the left column and those post dark etching for 1 h in 11 M NH_4F aqueous solutions containing (d) 0 (e) 1.0 (f) 5.0 M H_2O_2 with higher magnification (x 200 k) in the right column.

Figure 6 showed the cross-sectional SEM morphologies of the n-Si (100) after wet etching for 1 h in (a) 1.0 NH_4F, (b) 1.0 M NH_4F + 1.0 M H_2O_2, (c) 1.0 M NH_4F + 5.0 M H_2O_2 in contrast to those in (d) 11.0 NH_4F, (e) 11.0 M NH_4F + 1.0 M H_2O_2, (f) 11.0 M NH_4F + 5.0 M H_2O_2, respectively. It is evident that top-view morphologies shown in Figs. 4 and 5 are consistent with those depicted in Fig. 6 to confirm the fact that a single use of NH_4F solution (1.0 M or 11.0 M) doesn't result in any attack on the silicon surface whereas the combination of dilute NH_4F (1.0 M) and H_2O_2 (1.0 or 5.0 M) leads to a porous film produced on the silicon surface. The higher concentration of H_2O_2 in 1.0 M NH_4F, the

greater is the average diameter as well as the depth of the pore. Pore depth increases from 200 to 300 nm with increasing the H_2O_2 concentration from 1.0 to 5.0 M in 1.0 NH_4F. However, when a concentrated NH_4F solution (11.0 M) was mixed with H_2O_2 (1.0 or 5.0 M), only a rough surface was formed resultant from slightly uniform attack on the silicon. The effect of hydrogen peroxide is more significant that of fluoride in the mixed solution.
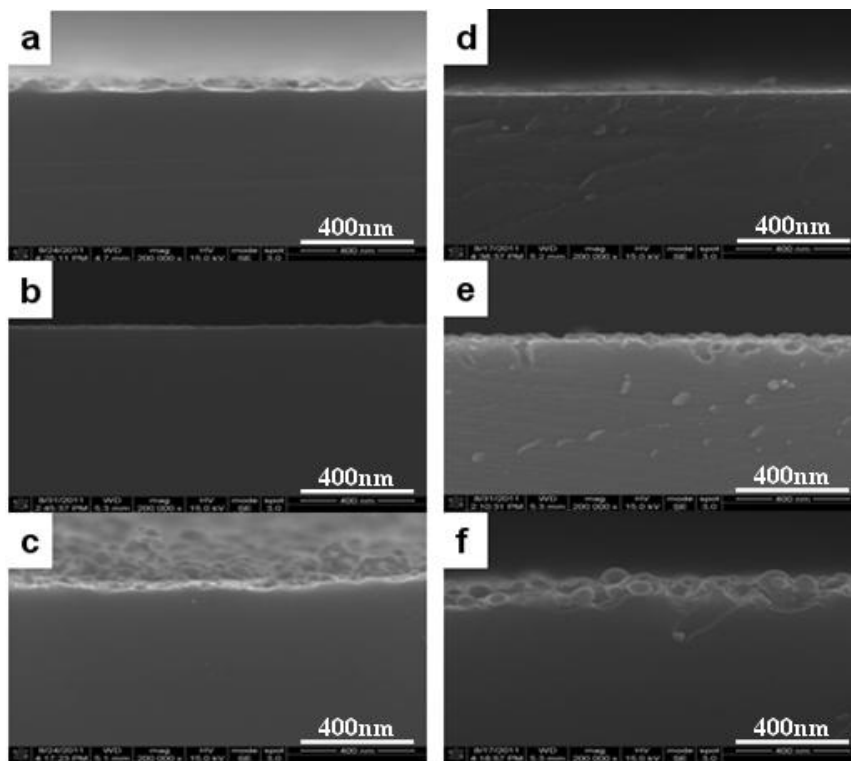

Figure 6. Cross-sectional views of SE morphologies for n-Si specimen after wet etching for 1 h in (a) 1.0 M NH_4F, (b) 1.0 M NH_4F + 1.0 M H_2O_2, (c) 1.0 M NH_4F + 5.0 M H_2O_2, (d) 11.0 M NH_4F, (e) 11.0 M NH_4F + 1.0 M H_2O_2, (f) 11.0 M NH_4F + 5.0 M H_2O_2, respectively. (x 200 k).

3.3. EIS of n-Si (100) at open circuit potential in 1.0 M NH_4F + 5.0 M H_2O_2 and in 11.0 M NH_4F + 5.0 M H_2O_2 systems

Electrochemical impedance spectroscopy (EIS) could provide useful information on the characteristics of interfaces, including the structure of interfacial layer, storage of charges in the electric double layer, and the resistance to charge transfer. The character can be changed, measured and analyzed the response caused by a very small perturbation to the system through a very wide range of frequency from 10^5 to 10^{-1} Hz.

Figure 7 depicted the EIS of n-Si (100) represented by Nyquist plots in the solution of (a) 1.0 M NH_4F without and with 5.0 M H_2O_2 and that in (b) 11.0 M NH_4F without and with 5.0 M H_2O_2, respectively. Comparing the real axes of the Nyquist plots in Figs. 7(a) and (b), we found that the polarization resistance is much greater at the interfaces between n-Si (100) and NH_4F solutions free from H_2O_2 than that in presence of it. This result indicated that in the presence of H_2O_2, the charge-

transfer resistance at the electrode interface was significantly reduced, thus facilitating the wet etching with formation of pores.
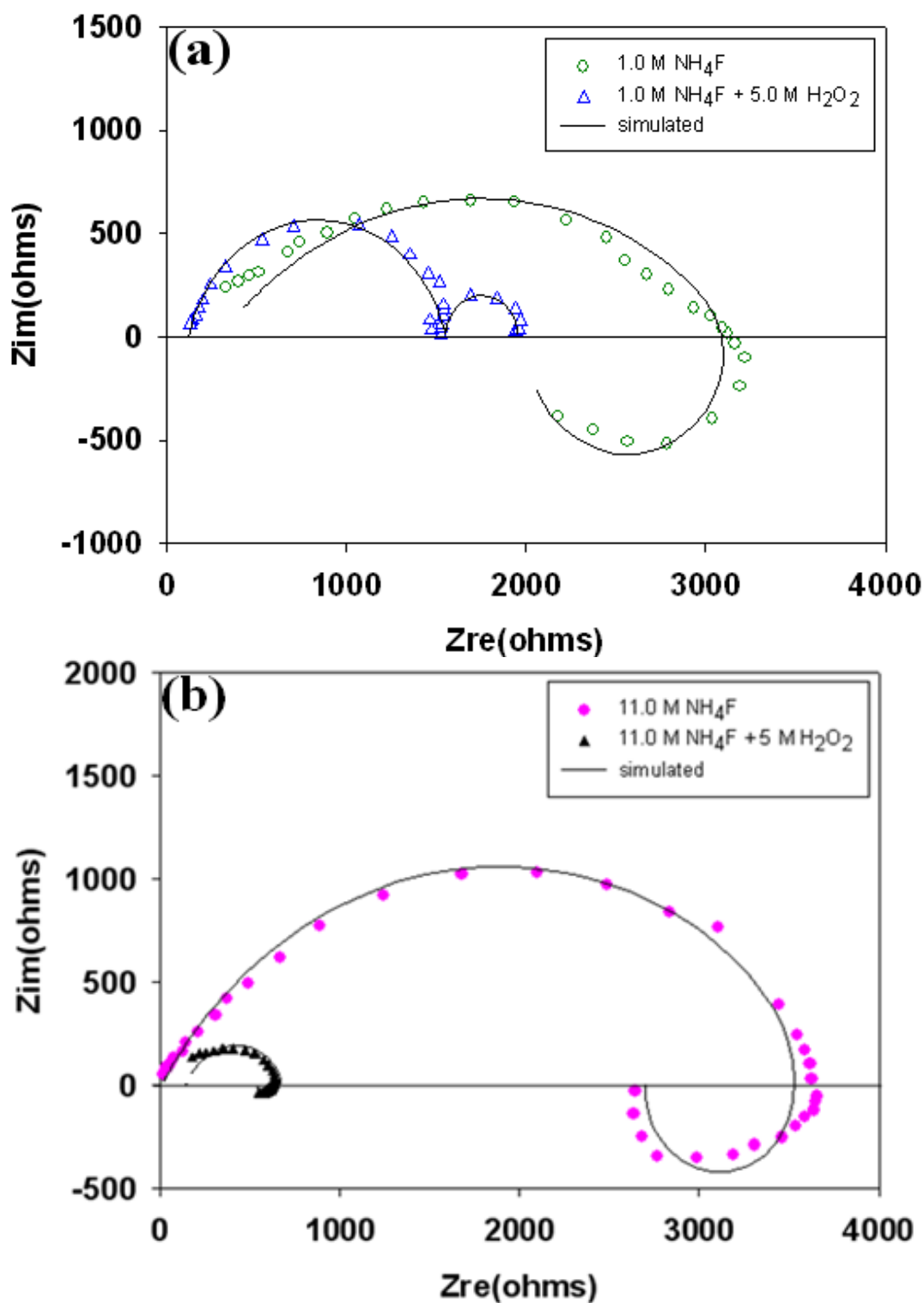

Figure 7. Nyquist plots for the wet etching of n-type silicon in the aqueous solutions of (a) 1.0 M NH$_4$F without and with 5.0 M H$_2$O$_2$, (b) 11.0 M NH$_4$F without and with 5.0 M H$_2$O$_2$.

By checking the Nyquist plots shown in Figs. 7(a) and (b), we found that the etching behavior of n-Si (100) in the solution of 1.0 M NH_4F, 11.0 M NH_4F, and 11.0 M NH_4F + 5.0 M H_2O_2 reveal the same profile : one path consisting of a capacitance arc in company of an induction loop at lower frequencies. The capacitance arc perhaps associated with the dissolution of silicon and the induction loop may be ascribed to adsorption and desorption on the silicon surface caused by dissolved silicon compounds. On the other hand, the Nyquist plot of n- Si (100) in the solution 1.0 M NH_4F + 5.0 M H_2O_2 displayed two distinct capacitance arcs. These two capacitance arcs are corresponding to porous formation through silicon dissolution and oxide layer formation on the silicon surface.

4. DISCUSSION

4.1 OCP of n-Si (100) in ammonium fluoride solutions influenced by hydrogen peroxide

As shown in Fig. 2, in the absence of hydrogen peroxide, the OCP of Si (100) is more active in 11.0 M than 1.0 M NH_4F solution. The addition of hydrogen peroxide leads to a shift of OCP to the noble direction. With increasing the concentration of H_2O_2, the OCP is higher. It has been well known that silicon (Si) and silica (SiO_2) suffer from dissolution in the fluoride solutions [18] and the dissolution rate depends upon their OCP in the solution. The OCP and the dissolution rate were influenced by the fluoride concentration, oxygen content, pH value and the convection of the solution [19]. The pH in 1.0 M NH_4F solution was measured at 4.8 and that in 11.0 M was at 8.0. In the presence of H_2O_2, the pH decreased a little (i.e. 4.6 in 1.0 M NH_4F + 1.0 M H_2O_2; 7.7 in 11.0 M NH_4F + 1.0 M; 4.4 in 1.0 M NH_4F + 5.0 M H_2O_2; 7.5 in 11.0 M NH_4F + 5.0 M H_2O_2). If n-Si (100) was immersed in dilute fluoride (i.e., 1.0 M NH_4F regardless without or with H_2O_2), the pH revealed slightly acidic; however, for the silicon immersed in the concentrated fluoride (i.e., 11.0 M NH_4F regardless without or with H_2O_2), the pH turned to slightly alkaline. In the acidic solution, the silicon surface inclined to terminate with hydrogen bond (i.e., Si-H) whereas it tended to terminate with hydroxyl bond (i.e., Si-OH) in the alkaline solution. It was reported that the silicon bonding with terminal hydrogen is much stable than with other terminal bond such as hydroxyl [20]. As a result, silicon surface terminal with hydroxyl bonds (i.e., in the single 11.0 M NH_4F) is less stable and more facilitates to dissolution than that terminal with hydrogen bond (i.e., in the single 1.0 M NH_4F). This fact can be confirmed by checking the SEM morphologies shown in Figs 4, 5 and 6 (a) and (d). It was also reported that the presence of hydrogen peroxide in the fluoride solutions would result in surface passivation [21] by means of bonding formation with terminal hydrogen. The higher concentration of hydrogen peroxide, the higher is the OCP responsible and the more passive is the silicon surface.

4.2 Detailed analysis of EIS data by proposed equivalent circuits

By running the software, Z-view, to proceed with the simulation based on a number set of proposed equivalent circuits standing for the possible mechanisms, we obtained a number of theoretical EIS curves those can fit to the experimental EIS data. Among those curves, we chose the

best fitting curve which corresponds to meaningful set of the equivalent circuit as the satisfactory solution. Figure 8 indicated two proposed sets of equivalent circuits whose theoretical EIS curves revealing the appropriate fit to the experimental data, as shown in Figs. 7(a) and (b), for the wet etching of n-Si (100) coated previously with sparse Ag-particles in different ammonium fluoride solutions. The set EQA depicted in Fig. 8(a) stands for the etching system in 1.0 M NH_4F without H_2O_2, 11.0 M NH_4F without H_2O_2 and 11.0 M NH_4F with 5.0 M H_2O_2. In contrast, the set EQB represents the etching in the solution of 1.0 M NH_4F with 5.0 M H_2O_2. In each set of equivalent circuit, it consists of a series of elements such as resistors (denoted as R), capacitors (denoted as C), and inductances (denoted as L) which were properly combined in parallel or in sequence to stand for a specific wet etching mechanism.

For understanding the contribution of these elements in the equivalent circuit to impedance of the system, we are going to detail the elements. In a common corrosion system, there exists a solution resistance (i.e., R_1) between the working electrode (i.e., n-Si) and the reference electrode (SCE). In addition, the electric double layer at the interface between n-Si (100) and electrolyte (i.e., ammonium fluoride solution) consists of a pseudo-capacitor (CPE1) and a charge-transfer resistor (R_2). In occasion, the presence of stable oxide may lead to an oxide capacitor (C_1) and a resistance (R_3) arisen from the oxide. Due to the reduction reactions of the oxidizer catalyzed by the silver nano-particles occurs continuously at the etching interface, the surface of the substrate is no longer flat and even. It was non-smooth surface may reveal a pseudo-capacitor rather than a capacitor in the equivalent circuit. Therefore, the combination of elements in the equivalent circuit EQB, as shown in Fig. 8 (b), stands for a corrosion system with stable oxide present on porous silicon. In contrast, under the condition where the oxide might turn into instable reaction intermediate, the oxide resistance (R_3) tends to shrinkage and the oxide capacitor (C_1) inclines to disappear but present with an inductance (L_1) which corresponds to adsorption and desorption of the unstable intermediate on the silicon surface. The equivalent circuit EQA shown in Fig. 8(a) is responsible for the system of silicon where the stable oxide disappeared but forming intermediates (F^-/SiF_4) instead in 11.0 M NH_4F with 5.0 M H_2O_2.

Non-smooth surface on the silicon should be ascribed to the reduction reactions of the oxidizer catalyzed by the silver nano-particles on etching interface. In addition, many products appear during the etching process (such as SiF_4), shifting the Nyquist plot from the ideal R-C mode [22-23]. The overall impedance Z could be estimated by using the formula below:

$$Z = R_1 + [\frac{R_2}{1 + (2\pi f R_2 CPE1)^\alpha}] \tag{1}$$

Where Z is the overall impedance of the system; R_1 represents the resistance of the etching solution; R_2 denotes charge transfer resistance; CPE_1 is the psudo-capacitance of the electric double layer; f represents the frequency, and α is an empirical constant correcting changes in surface composition according to the duration of etching, usually ranging between 0 and 1. In general, the value of Z changes with the duration of etching so that results in more distinctive variation of the characteristic phase angle with time. The results from the simulated equivalent circuit are listed in Table 1.
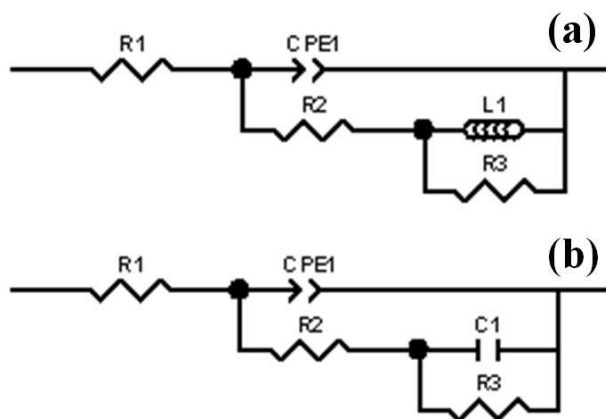
Figure 8. Equivalent circuits proposed to govern the dark etching of n-Si deposited previously with sparse Ag-particles in (a) 1.0 M NH$_4$F without H$_2$O$_2$, 11.0 M NH$_4$F without H$_2$O$_2$ and 11.0 M NH$_4$F with 5.0 M H$_2$O$_2$ and (b)1.0 M NH$_4$F with 5.0 M H$_2$O$_2$ solution.

Table 1. EIS data simulated on the basis of the equivalent circuits proposed in Fig. 8(a) and (b), respectively.

etch conditions		element conditions							
solution	H$_2$O$_2$(M)	OCP(mV)	R$_1$(Ω)	CPE$_1$-T(F)	α	R$_2$(Ω)	L$_1$(H)	R$_3$(Ω)	C$_1$(F)
1.0 M NH$_4$F	0	-406	300	1.0E-06	0.55	1700	50	1200	N
1.0 M NH$_4$F	5	-367	125	6.7E-07	0.85	1430	N	400	0.01
11.0 M NH$_4$F	0	-431	5	1.6E-06	0.65	2700	40	1100	N
11.0 M NH$_4$F	5	-384	180	6.1E-06	0.80	400	2.5	175	N

4.3 Schematic model for the wet etching of Ag-particles coated n-Si (100) in ammonium fluoride solutions with and without H$_2$O$_2$

As mentioned earlier that almost all the mechanism for the wet etching of silicon coated with sparse silver nano-particles had been focused on p-type Si despites whether or not a presence of anodic bias [24]. As for n-type Si, electrochemical etching under illumination in hydrogen fluoride without [25] and with ethanol [14] was well discussed. However, seldom report regarding wet etching of the n-silicon coated with sparse silver nano-particles in the dark was found. It is conceivable that the presence of oxidizers (such as hydrogen peroxide in the work) of significance. It has been reported and generally believed that hydrogen peroxide in the etching solutions is catalyzed by metallic silver particles on the silicon to facilitate the etching reaction thus accelerating pores formation by obeying the following equation

$$H_2O_2 + 2\,H^+ \rightarrow 2\,H_2O + 2\,h^+ \qquad\qquad (2)$$

According to eq (2), two moles of positive holes are produced on the silver particles by consuming of 1 mole H$_2$O$_2$. The positive holes rapidly transfer through the silver particles into the Si-substrate at the periphery aroud the Ag-particles. In contrast, surface of Si (100) free from covering by

Ag-particles will suffer oxidation to form oxide film (i.e., to be terminated with –SiO), as depicted in Fig. 9 (a), following the equation

$$Si + 2H_2O_2 \rightarrow SiO_2 + 2\ H_2O \tag{3}$$

The oxide film on the silicon will be very thin and instable thus tending to dissolution in usual hydrogen flouride and concentrared ammonium flouride solution (11.0 M). However, it is thicker and stable in dilute ammonium fluorde (like 1.0 M) thus suffering only slighly dissolution.

On the other hand, for receiving the positive holes from Eq (2) via Ag-particles, the silicon under the Ag-particles periphery may give rise to dissolution in the fluoride solution as follows

$$Si + 4h^+ + 4\ HF \rightarrow SiF_4 + 4H^+ \tag{4}$$

$$SiF_4 + 2\ HF \rightarrow H_2SiF_6 \tag{5}$$

The formulas above reveal that the dissolution of silicon requires the participation of electron holes; in the absence of applied bias voltage and light irradiation, electron holes can only originate from the catalysis of silver particles.
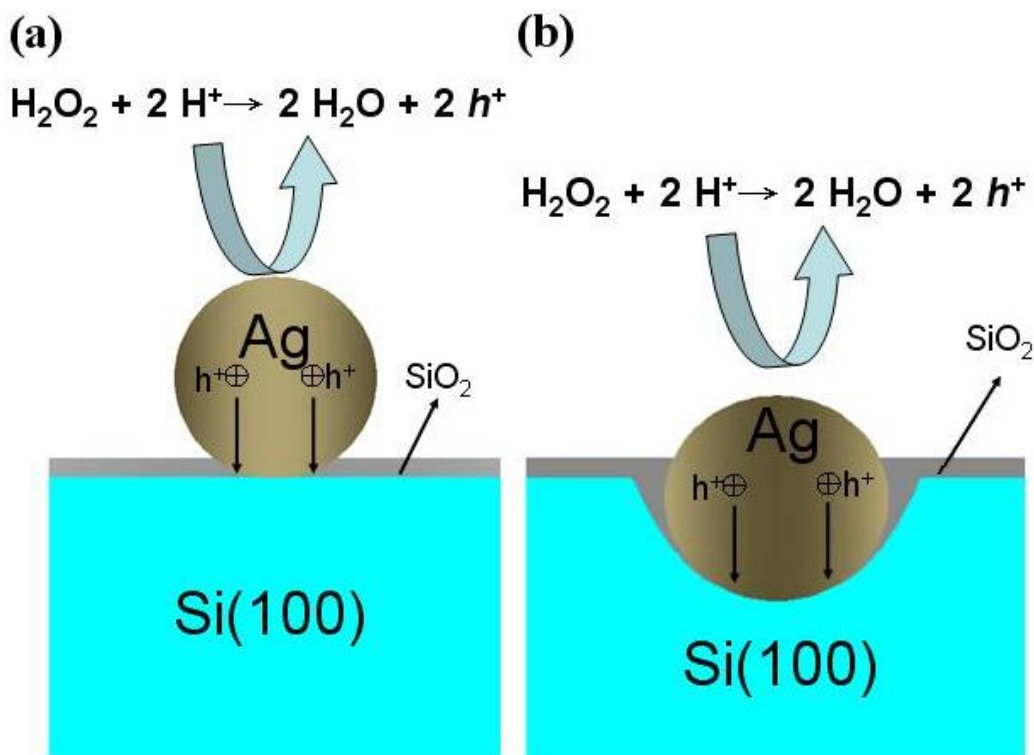

Figure 9. Schematic model for the dark etching of n-type silicon deposited previously with sparse Ag-particles in the ammonium fluoride aqueous solutions

The coating of silver nano-particles on the wafer can be regarded as the cathode and the surface of the silicon can be regarded as the anode [26]. However, in the NH_4F/H_2O_2 system, the reaction at the cathode involves the continuous reduction of hydrogen peroxide, during which the electron holes h^+ required for etching are produced. The electron holes drift away from the substrate to the interface between the silicon and the solution where they are injected into the silicon surface.

Since the species H_2SiF_6 is soluble in the aqueous solution, dissolving out of H_2SiF_6 from the peripheries of Ag-particles results in inlay of Ag-particle into the silicon substrate.

The contact periphery between silicon and Ag-particle may be influenced by H_2O_2 to receieve positve holes or suffer oxidation. Irrespective the silicon recieving the positive holes or the silicon oxide oxidized by H_2O_2, they are subject to dissloution in the fluordie solutions. This dissolution process in 1.0 M NH_4F + 5.0 M H_2O_2 may continue to form porous surface on the n-Si (100), as shown in Fig. 9 (b). In the system of 11.0 M NH_4F + 5.0 M H_2O_2, the oxide film on silicon surface free from covering by Ag-particles is so unstable that also suffering attack by the concentrated fluoride solution. In the alkaline 11.0 M NH_4F solution, there is no mush surpior for the dissolution rate of silicon to the ecting rate of the silicon oxide. As a result, only very shallow pores can formed on the Si (100). In the absence of H_2O_2, no possbility of positive holes can be produced so that the dissolution of silicon under Ag-paricles is difficult to undergo. According, no pores can be observed on the Si (100) surface in ethier single 1.0 M or 11.0 NH_4F solution.

4.4 Confirmation of the etching kinetic with the plots of phase angles

For confirming the etching kinetics interpreted by means of the Nyquist plots shown in Fig. 7, we consulted the EIS data again whereas by another type of plot. Fig. 10 exhibited the plots of phase angle against frequency for n-Si (100) in the solutions of (a) 1.0 M NH_4F and 1.0 M NH_4F + 5 M H_2O_2, and those in the solutions of (b) 11.0 M NH_4F and 11.0 M NH_4F + 5 M H_2O_2. It is apparent that the interface in 1.0 M NH_4F + 5.0 M H_2O_2 presents two time-constant spectra at both high and low frequencies, respectively indicating the generation of an oxide layer on the surface of the substrate and the occurrence of an etching reaction at the controlled interface [13]. Both are mutually competitive and co-exist. Previous studies also indicated the formation of oxide layers in ammonium fluoride solutions depending upon the fluoride concentrations. At concentrations less than 10%, the thickness of the oxide layer is proportional to the concentration of the fluoride solutions. However, at concentrations exceeding 10%, dissolution occurs more rapidly than the formation of the oxide layer, thus precluding the formation of oxides [27]. In contrast, the etching solution free from H_2O_2 does not reveal these two distinct signals. Figure 10(b) depicted the plots of phase angles for n-Si (100) in both 11.0 M NH_4F and 11.0 M NH_4F + 5 M H_2O_2 solution. It is clear that no distinct signals are produced at either high or low frequencies. This fact implies that the silicon is simply subject to corrosion without formation of any oxide layer on the surface.
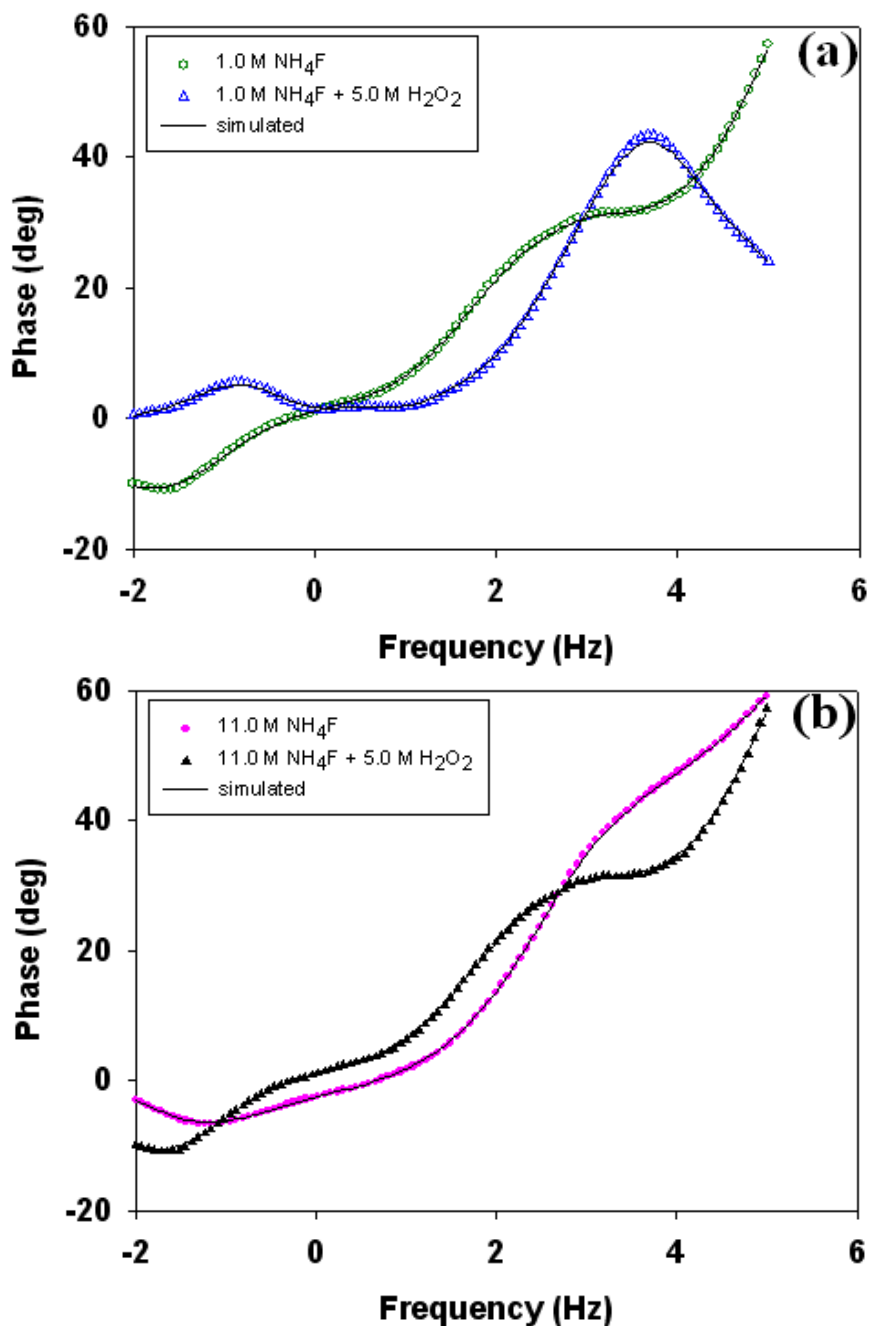
Figure 10. Plots of phase angle against logarithm scale of frequency for the dark etching of n-type silicon in the solutions of (a) 1.0 M NH_4F without and with 5.0 M H_2O_2, (b) 11M NH_4F without and with 5.0 M H_2O_2.

5. CONCLUSIONS

Wet etching of n-silicon coated with sparse silver nano-particles was carried out in ammonium fluoride solution with and without the presence of hydrogen peroxide in the dark. Ammonium fluoride is less reactive than hydrogen fluoride. In the absence of H_2O_2, the OCP of n-Si (100) in 11.0 M was more negative than in 1.0 M NH_4F. In the present of H_2O_2, the OCP moved to higher potential with

increasing the concentration of H_2O_2 (from 1.0 to 5.0 M). Examination by SEM, the smooth surface of n-Si (100) was etched in 1.0 M NH_4F + 5.0 M H_2O_2 for 1 h to form a porous surface where the pores were 50 - 150nm in diameter and 200 - 300nm in depth; In contrast, only a few shallow pores on the Si (100) surface could be formed after the etching conducted in 11.0 M NH_4F + 5.0 M H_2O_2 for 1 h. The study of electrochemical impedance spectroscopy (EIS) provided useful information to understand the kinetics of this system. Through simulation with commercial software (i.e., Z-view), two satisfactory sets of equivalent circuit (i.e., EQA and EQB) are proposed to realized the etching mechanism. With the aid of these two sets of equivalent circuit, the reaction mechanism could be illustrated by a schematic diagram. This mechanism could be reconfirmed to have two time constants by checking the plots of phase angle against the exerted frequencies (in logarithmic scale).

References

1. A.Uhlir, *The Bell system technical journal*, 35 (1956) 333.
2. V. Lehmann, H. Foll, *J. Electrochem. Soc.*, 137 (1990) 653.
3. H. Ohji, P. T. J. Gennissen, P. J. French, K. Tsutsumi, *J. Micromech. Microengin.*, 10 (2000) 440.
4. H. Ohji, P. J. Trimp, P. J. French, *Sensors and Actuators A:Physical*, 73 (1999) 95.
5. J. A. Walker, *J. Micromech. Microengin.*, 10 (2000) R1.
6. J. von Behren, L. Trubeskov, P. M. Fauchet, *App. Phys. Lett.*, 66 (1995) 1662.
7. R. Angelucci, A. Poggi, L. Dori, *Sensors and Actuators A:Physical*, 74 1 (1999) 95.
8. X. Li, P. W. Bohn, *App. Phys. Lett.*, 77 (2000) 2572.
9. R. Douani, T. Hadjersi, R. Boukherroub, L. Adour, A. Manseri, *App. Surf. Sci.*, 254 (2008) 7219.
10. Z. Huang, T. Shimizu, S. Senz, Z. Zhang, N. Geyer, Ulrich Go¨sele, *J. Phys. Chem. C*, 114 (2010) 10683.
11. V. A. Sivakov, G. Bro¨nstrup, B. Pecz, A. Berger, G. Z. Radnoczi, M. Krause, S. H. Christiansen, *J. Phys. Chem., C*, 114 (2010) 3798.
12. S. Bauer, J. G. Brunner, H. Jha, Y. Yasukawa, H. Asoh, S. Ono, H. Bohm, J. P. Spatz, P. Schmuki, *Electrochem Commun.*, 12 (2010) 565.
13. W. A. Badawy, R. M. El-Sherif, S. A. Khalil, *Electrochimica Acta*, 55 (2010) 8563.
14. J. C. Lin, C. M. Lai, W. D. Jehng, K. L. Hsueh, S. L. Lee, *J. Electrochem. Soc.,* 155 (2008) D436.
15. F. Yang, K. Roodenko, K. Hinrichs, J. Rappich, *J. Micromech. Microengin.*, 17 (2007) S56.
16. S. E. Bae, C. W. Lee, *The Electrochemical Society*, Inc., Abs. 6, 205th Meeting, (2004).
17. M. Lublowz, H. J. Lewerenz, *Electrochemical and Solid-State Letters*, 10 (2007) C51.
18. J. H. Ouyang, X. S. Zhao, T. Li, D. C. Zhang, *J. App. Phys.*, 93 (2003) 4315.
19. D. R. Turner, *J. Electrochem. Soc.*, 107 (1960) 810.
20. P. Jakob, Y. J. Chabal, *J. Chem. Phys.,* 95 (1991) 2897.
21. M. L. Chourou, K. Fukami, T. Sakka, S. Virtanen, Y. H. Ogata, *Electrochimica Acta*, 55 (2010) 903
22. A.E. Bohe, J. R. Vilche, K. Jüttner, W. J. Lorenz, W. Paatsch, *Electrochimica Acta*, 34 (1989) 1443.
23. R. M. El-Sherif, S. A. Khalil, W. A. Badawy, *J. Alloys and Compounds*, 509 (2011) 4122.

24. K. A. Salman, Z. Hassan, K. Omar, *Int. J. Electrochem. Sci.*, 7 (2012) 376.
25. W. D. Jehng, J. C. Lin, S. L. Lee, *J. Electrochem. Soc.*, 152 (2005) C124.
26. X. H. Xia, C. M. A. Ashruf, P. J. French, J. J. Kelly, *Chem. Mater.*, 12 (2000) 1671.
27. M. Niwano, Y. Kondo, Y. Kimura, *J. Electrochem. Soc.*, 147 (2000) 1555.